

Coupled guide and cavity in a two-dimensional photonic crystal

C. J. M. Smith^{a)} and R. M. De La Rue

Optoelectronics Research Group, Glasgow University, Glasgow G12 8LT, Scotland

M. Rattier, S. Olivier, H. Benisty, and C. Weisbuch

Laboratoire Physique de Matière Condensée, Ecole Polytechnique, Palaiseau 91128 Cedex, France

T. F. Krauss

School of Physics and Astronomy, University of St. Andrews, St. Andrews KY16 9SS, Scotland

R. Houdré and U. Oesterle

IMO, Ecole Polytechnique Fédérale de Lausanne, Lausanne CH-1015, Switzerland

(Received 21 August 2000; accepted for publication 19 January 2001)

We demonstrate, in a planar two-dimensional (2D) configuration, in the optical regime a clear association of two photonic crystal elements and the ability to produce a low-loss coupled system. A channel waveguide is brought to between two and five crystal rows (450 to 1126 nm) from a 2D microcavity fabricated in a GaAs/AlGaAs waveguide. We probe these two elements individually and explore their interaction. © 2001 American Institute of Physics. [DOI: 10.1063/1.1355667]

Photonic crystals (PCs) are recognized for their potential as a platform for realizing compact and highly functional optoelectronic circuits in both two (2D) and three dimensions (3D).^{1,2} Planar 2D structures have received much attention because they are easier to fabricate yet provide most of the functionality of 3D structures.^{3–8} Recently, groups worldwide have looked at PC cavities^{9–11} and waveguides,^{6,8,12–14} essential elements for future photonic integrated circuits. We show here the integration of two elements—a photonic crystal channel waveguide (PC-WG) and a photonic crystal microcavity (PC-MC)—which marks an important development in this field. We show that the nature of the PC-WG gives rise to an unusual type of mode coupling that proves effective in coupling the microcavity to the waveguide. Moreover, we show that the interaction satisfies an important requirement for photonic integrated circuits—the capacity to couple various elements with minimal losses.

The structures are fabricated in a waveguide consisting of a GaAs core and asymmetric AlGaAs cladding layers.¹⁵ Three layers of InAs quantum dots, located in the center of the core, have a large distribution of dot sizes and, hence, a broad photoluminescence (PL) spectrum [920–1060 nm (Ref. 15)]. The PC patterns, with a period of 260 nm and hole diameter of 170 nm, are generated using electron-beam lithography (Fig. 1). Reactive-ion etching is used to transfer the pattern through the waveguide core to a total etch depth of 0.8 μm .¹⁶ The PC-MC has an area of 8.6 μm^2 and the PC-WG is 0.61 μm wide. PL is excited with a 3 μm diameter laser spot that can be positioned to any location¹⁷ allowing us to excite either at the guide entrance (E1) or inside the cavity (E2) (Fig. 1). Also, we can detect either the PL emitted normal to the sample surface on either side of the cavity (S2 or S3)¹⁸ or the transverse electric (TE)-polarized PL that

exits from the cleaved edge, provided that it is located within 100 μm of the patterns (S1) (Fig. 1).¹⁷ The 2D photonic crystal only provides an in-plane photonic band gap for TE polarization and we measure only this polarization.

Previously, we have investigated isolated microcavities of the same type⁹ in the E2–S3 configuration and observed that the 3D confinement provided by these cavities is good. Peaks with resolution-limited linewidths ($Q = \lambda/\Delta\lambda \sim 1000$) gave direct evidence of the discrete PC-MC modes. Similar spectral features are observed here when the waveguide is five rows from the microcavity [Fig. 2(f)]. We attribute the observed modes to “quasi-radial”¹⁸ or “Fabry–Perot”^{10,11,19} resonances of the cavity, with wave fronts parallel to the cavity boundary, giving rise to a significant scattered far field in the air.²⁰

Recently, we have measured the properties of PC-WGs in the E1–S1 configuration²¹ and observed transmission

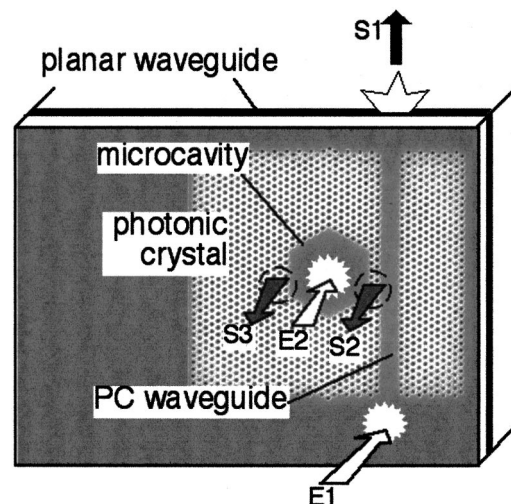


FIG. 1. Localized PL setup showing the different excitation points either near the guide entrance (E1) or in the microcavity (E2). Collection from both the cleaved edge (S1) and through the excitation objective (S2 and S3) is used. Scanning electron microscopy micrograph image is for 260 nm period photonic crystal.

^{a)}Present address: Intense Photonics Ltd., Block 7 Kelvin Campus, West of Scotland Science Park, Glasgow G20 0TH, Scotland, UK; electronic mail: chris_smith@intensephotonics.com

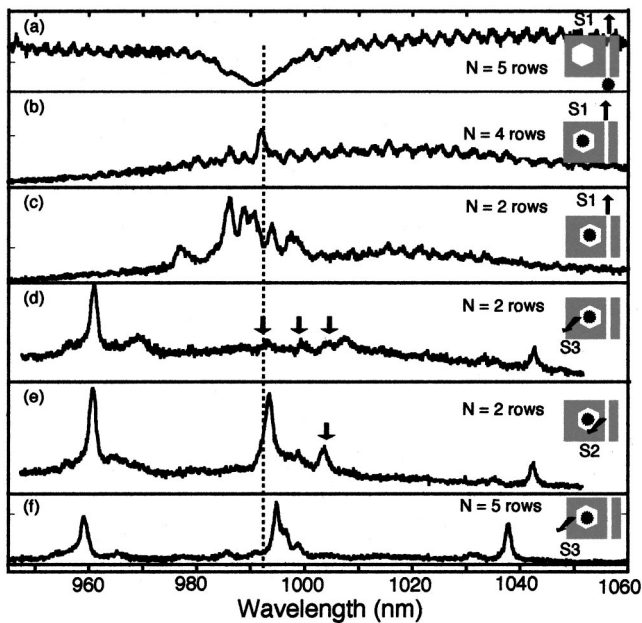


FIG. 2. Spectra for the uncoupled [(a) and (f)] and the coupled [(b)–(e)] elements. (a) Signal S1 for excitation near the waveguide entrance (E1) and $N=5$ rows. The fast oscillations are the Fabry–Perot fringes between the cleaved edge and the PC. Signal S1 for excitation in the PC-MC (E2), and (b) $N=4$ rows, and (c) $N=2$ rows. (d) Signal S3 and (e) S2 for excitation in the PC-MC and a strongly coupled case ($N=2$ rows). (f) Signal S3 for $N=5$ rows, the reference “uncoupled” PC-MC. All clusters have similar intensities.

properties that depend strongly on the periodic nature of the waveguide boundaries. Energy traveling forward in the fundamental TE mode couples to one of the backward propagating higher-order modes by means of the periodic perturbation introduced by the PC-WG boundary, with momentum conservation being achieved by the reciprocal lattice vector of magnitude $2\pi/a$. As a result, a narrow ministopband that stems from the anticrossing of these two coupled modes was seen in the waveguide transmission spectrum. An identical spectral feature is observed for the present PC-WG when there are five rows of photonic crystal between the PC-WG and PC-MC [Fig. 2(a)]. Clearly, the intrinsic characteristics of these two elements are well defined even when in relatively close proximity ($1.12\ \mu\text{m}$ separation). If we now excite inside the cavity but bring the waveguide to within four rows of the microcavity, light is coupled from the PC-MC into the PC-WG as shown by the extra peaks in the spectrum [Fig. 2(b)]. If the distance is decreased to two rows, the peaks are larger and more numerous, i.e., coupling is stronger [Fig. 2(c)].

There is a number of striking features in these observations: (i) Coupled peaks in the waveguide transmission are only observed in the 980–1000 nm wavelength range that corresponds to the spectral position of the ministopband of the PC-WG of Fig. 2(a). (ii) The number (~ 6) of observed modes in this 20 nm wide range is close to the estimate of the 2D density of states using the bare PC-MC area (eight expected peaks).²² (iii) The observed quality factors, Q , are constant, regardless of the separation between the PC-WG and PC-MC. As for their absolute value, we are limited by the resolution of the spectrometer—so that actual Q values are above $Q \sim 1000$. It should be noted that the slight varia-

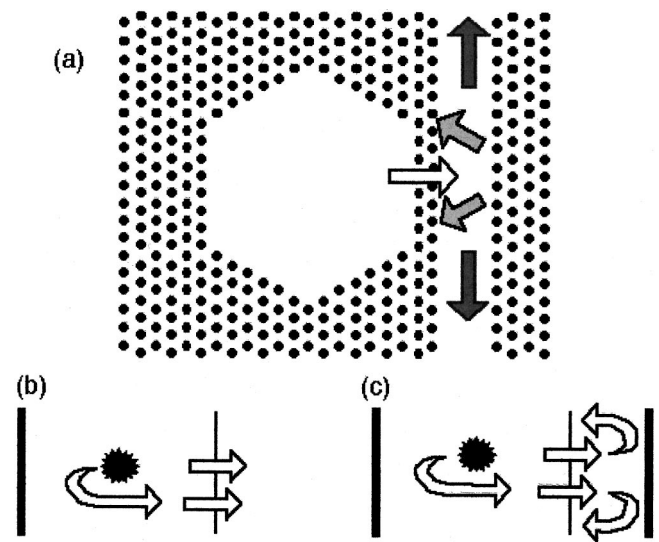


FIG. 3. (a) Schematic of coupling mechanism: energy radiates across the intermediate boundary (white arrow), where it can couple to the higher order modes of the waveguide (gray arrows), that can then couple to the fundamental mode (black arrows) by means of the waveguide anticrossing mechanism. Schematic showing (b) open microcavity and (c) microcavity with far wall that is essential to the production of a coupled system and observation of these modes through the anticrossing mechanism.

tions in the spectral position of the peaks are due to fabrication fluctuations.

Observation (i) clearly indicates that the coupling between the two elements is due to the anticrossing mechanism that was observed for the waveguide. Indeed, the cavity modes radiate preferentially through the wall with a large transverse momentum (transverse with respect to the waveguide propagation axis), namely they couple to the higher order transverse mode of the waveguide. This higher order mode then couples to the fundamental mode via the anticrossing mechanism [Fig. 3(a)]. It should be noted that the distance between the waveguide exit and the middle of the guide, and hence the microcavity, is short enough (only 18 rows) so that sizeable transmission is obtained while the slow group velocity of higher order mode ensures good conversion between the higher order and fundamental mode. The density of the peaks, observation (ii), suggests that any cavity mode with a transverse momentum will be coupled to the PC-WG, with varying but sizeable efficiency.

Finally, the fact (iii) that the cavity Q values do not degrade as the interaction is increased suggests that the resonant modes observed are those of the coupled cavity-waveguide system. We have stated in (ii) that the interaction between the waveguide and the cavity is via the interaction of the cavity quasi-radial modes and the higher transverse order mode of the waveguide. In the first instance, consider the simple transfer of energy from the microcavity if we were to replace the guide with the continuum. We represent this case in Fig. 3(b) as a 1D system, since the wave fronts of the modes of interest are almost normal to the confining boundaries. The two rows of the coupling PC region have a transmission in the 40% range ($R \sim 60\%$) so one would expect to observe a quality factor $Q \sim 400$ for the cavity modes, as deduced from a ray tracing approach. As we observe $Q > 1000$, there is no doubt that the observed quasi-radial modes¹⁸ “see,” in the coupled system, the boundary of the

waveguide opposite to the cavity [Fig. 3(c)]. The leakage to another *highly reflective* PC mirror does not degrade the cavity Q below our resolution limit. This means that systems such as the one considered here do indeed work in the mutual coupling regime, energy being exchanged between the waveguide and microcavity.

Furthermore, the mixture of the cavity modes with the local waveguide modes that we observe here is another signature of the coupled system. When scattered light was collected either on the cavity edge opposite to the guide [S3 in Fig. 1 and spectrum of Fig. 2(d)] the spectra were distinctly different. In the S2 signal, one unambiguous additional peak is seen at 1004 nm, corresponding to a resonant mode of the mutual system possessing a large field intensity in the separation. The same peak is also seen when exciting PL inside the PC-WG itself and detecting the S3 signal, thereby assessing the coupled nature of the system. On the opposite side (S3), not only does this peak disappear, but all the peaks in the region of good coupling are depleted, including the largest 993 nm peak, which is thus also a peak of the coupled system (see arrows). This observation means that light travels predominantly across the microcavity-waveguide boundary and flows eventually into the guide, thereby depleting the field on the other sides of the cavity.

The system presented has thus demonstrated that PC elements can form a coupled system with minimal losses. Moreover, with individual elements and their interaction now demonstrated, the door has been opened to integration on a much larger scale, and the prospects for integrated optical circuits based on photonic crystals have moved an important step closer to reality. The large signals observed in the present experiments clearly show that there is a significant transfer of energy between the cavity and propagating waveguide modes. The next step will be to study what kind of coupler and cavity geometry give rise to better control in coupling to the propagating modes of the photonic crystal waveguide, not only at frequencies around but also at frequencies away from the anticrossing region. Such control is one of the main issues in engineering photonic devices, such as add-drop filters and multiplexers, and more general circuits based on photonic crystals.

The authors would like to acknowledge the support of the Nanoelectronics Research Centre and the Dry Etch Group at Glasgow University. This work was supported by

the UK EPSRC and EU ESPRIT projects SMILED and PICCO; one of the authors (T.F.K.) is supported by a Royal Society Research Fellowship.

- ¹J. D. Joannopoulos, R. D. Meade, and J. N. Winn, *Photonic Crystals* (Princeton University Press, Princeton, NJ, 1995).
- ²R. D. Meade, A. Devenyi, J. D. Joannopoulos, O. L. Alerhand, D. A. Smith, and K. Kash, *J. Appl. Phys.* **75**, 4753 (1994).
- ³P. R. Villeneuve, S. Fan, S. G. Johnson, and J. D. Joannopoulos, *IEE Proc. J: Optoelectron.* **145**, 384 (1998).
- ⁴O. Painter, J. Vuckovic, and A. Scherer, *J. Opt. Soc. Am. B* **16**, 275 (1999).
- ⁵H. Benisty, C. Weisbuch, D. Labilloy, M. Rattier, C. J. M. Smith, T. F. Krauss, R. M. De La Rue, R. Houdre, U. Oesterle, C. Jouanin, and D. Cassagne, *J. Lightwave Technol.* **17**, 2063 (1999).
- ⁶M. D. B. Charlton, M. E. Zoorob, G. J. Parker, M. C. Netti, J. J. Baumberg, S. Cox, and H. Kemhadjian, *Mater. Sci. Eng. B* **74**, 17 (2000).
- ⁷S. G. Johnson, S. H. Fan, P. R. Villeneuve, J. D. Joannopoulos, and L. A. Kolodziejski, *Phys. Rev. B* **60**, 5751 (1999).
- ⁸M. C. Netti, M. D. B. Charlton, G. J. Parker, and J. J. Baumberg, *Appl. Phys. Lett.* **76**, 991 (2000).
- ⁹C. J. M. Smith, H. Benisty, D. Labilloy, U. Oesterle, R. Houdre, T. F. Krauss, R. M. De La Rue, and C. Weisbuch, *Electron. Lett.* **35**, 228 (1999).
- ¹⁰P. Pottier, C. Seassal, X. Letartre, J. L. Leclercq, P. Viktorovitch, D. Cassagne, and C. Jouanin, *J. Lightwave Technol.* **17**, 2058 (1999).
- ¹¹O. J. Painter, A. Husain, A. Scherer, J. D. Obrien, I. Kim, and P. D. Dapkus, *J. Lightwave Technol.* **17**, 2082 (1999).
- ¹²T. Baba, N. Fukaya, and J. Yonekura, *Electron. Lett.* **35**, 654 (1999).
- ¹³M. Tokushima, H. Kosaka, A. Tomita, and H. Yamada, *Appl. Phys. Lett.* **76**, 952 (2000).
- ¹⁴S. Y. Lin, E. Chow, S. G. Johnson, and J. D. Joannopoulos, *Opt. Lett.* **25**, 1297 (2000).
- ¹⁵D. Labilloy, H. Benisty, C. Weisbuch, C. J. M. Smith, T. F. Krauss, R. Houdre, and U. Oesterle, *Phys. Rev. B* **59**, 1649 (1999).
- ¹⁶T. F. Krauss, C. J. M. Smith, B. Vogeles, S. K. Murad, C. D. W. Wilkinson, R. S. Grant, M. G. Burt, and R. M. De La Rue, *Microelectron. Eng.* **35**, 29 (1997).
- ¹⁷D. Labilloy, H. Benisty, C. Weisbuch, T. F. Krauss, R. Houdre, and U. Oesterle, *Appl. Phys. Lett.* **71**, 738 (1997).
- ¹⁸D. Labilloy, H. Benisty, C. Weisbuch, T. F. Krauss, C. J. M. Smith, R. Houdre, and U. Oesterle, *Appl. Phys. Lett.* **73**, 1314 (1998).
- ¹⁹R. K. Lee, O. J. Painter, B. Durso, A. Scherer, and A. Yariv, *Appl. Phys. Lett.* **74**, 1522 (1999).
- ²⁰J. M. Gérard, D. Barrier, J. Y. Marzin, R. Kuszelewicz, L. Manin, E. Costard, V. Thierry Mieg, and T. Rivera, *Appl. Phys. Lett.* **69**, 449 (1996).
- ²¹C. J. M. Smith, H. Benisty, M. Rattier, S. Olivier, T. F. Krauss, R. M. De La Rue, R. Houdre, U. Oesterle, and C. Weisbuch, *Proceedings of the International Workshop on Photonic and Electromagnetic Structures, Sendai, Japan, 8–10 March 2000*.
- ²²For a sixfold symmetric dielectric function $\epsilon(x,y)$, the modal degeneracy is the same as that of the benzene molecule: one half of the eigenfrequencies is doubly degenerate. This is taken into account in the present density-of-states estimate.